

PAPER • OPEN ACCESS

Increasing yield of graphene synthesis from oil palm empty fruit bunch via two-stages pyrolysis

To cite this article: P Widiatmoko *et al* 2019 *IOP Conf. Ser.: Mater. Sci. Eng.* **543** 012032

View the [article online](#) for updates and enhancements.



IOP | ebooks™

Bringing you innovative digital publishing with leading voices to create your essential collection of books in STEM research.

Start exploring the [collection](#) - download the first chapter of every title for free.

Increasing yield of graphene synthesis from oil palm empty fruit bunch via two-stages pyrolysis

P Widiatmoko, I F Sukmana, I Nurdin, T Prakoso and H Devianto

Institut Teknologi Bandung, Jl. Ganesha 10, Bandung, 40132, Indonesia

E-mail: pramujo@che.itb.ac.id

Abstract. Graphene is a 2D hexagonal lattice structure of sp^2 carbon atoms which has been acknowledged for its superior electrical, mechanical, and thermal properties. Production of graphene in large scale and low cost are attracting topic in recent years. Previous study shows that production of graphene from biomass via pyrolysis has low yield of graphene. In this study, we produced graphene sheets from oil palm empty fruit bunch via two-stages pyrolysis to increase the yield. The produced graphene sheets were characterized by scanning electron microscopy, transmission electron microscopy, Raman scattering, and X-ray diffraction. Surface properties (i.e. effective surface areas, pore volumes, and pore size distributions) were studied by nitrogen adsorption-desorption measurements. Effect of the first stage temperature of pyrolysis on the yield, structure, and properties of graphene has been investigated. Our result indicated that two-stages pyrolysis could increase the yield of graphene up to 70%. Graphene sheets shows favorable features of nanosheet frameworks (4–10 atomic layers) and high surface area ($870 \text{ m}^2 \text{ g}^{-1}$).

1. Introduction

Indonesia is well known as the largest producer and exporter of palm oil in the world. The directorate general of plantation (Indonesia) recorded that in 2015, Indonesia produces 31 million tons of crude palm oil (CPO). Production of the CPO increased from 5.39 to 8.42% per year in term of 2010 to 2015. Processing oil palm fresh fruit bunch (FFB) into CPO result in abundant biomass by-products such as empty fruit bunch, oil palm kernel, and palm oil milling effluent. The produced CPO is only about 30% of the FFB mass, while the rest will become waste of biomass. High content of organic material in the by-product of oil palm milling may harmful to environment. Therefore, proper treatment is required. Recently, biomass is considered as a promising source of energy or biofuels, chemicals, and bio-based products which will reduce the dependency on fossil fuels [1]. Charcoal and activated carbon are industrial example of the biomass-based products. Another promising high value product from the biomass is graphene.

Graphene is a thin sheet of carbon which has high conductivity, large surface area [2]. The graphene has been widely applied in nanoelectronic and nanocomposite components such as transistors, solar cells, molecular sensors, and lithium ion batteries. In addition, graphene can also be utilized as a sturdy electrode material for supercapacitors [3]. Supercapacitor is an emerging technology on electrical energy storage. The supercapacitor utilizes large electrode surface and electrical double layer which allows it to possess greater energy density than the conventional capacitors as well as much greater power density than the batteries [4].

Study on graphene synthesis using biomass precursors has been done previously. Shams et al. [5] have made graphene from dried camphor leaf precursors by pyrolysis method at a temperature of 1200°C



with yield of about 0.8%. Graphene has also been produced from palm empty fruit bunches (EFB) and palm kernel shells by pyrolysis method at 900°C with yield of fixed carbon is about 27%. Higher yield of graphene, therefore, is desired from the process. In this study, we utilize two-stages pyrolysis for obtaining higher graphene yield. The idea is to exploit different decomposition temperature of cellulose, hemicellulose, and lignin as main structure of the EFB.

2. Methods

2.1. Graphene synthesis

Dried EFB was crushed using ball mill and then sieved into coarse granules (170-200 mesh). The prepared raw material was mixed with 3M FeCl₃ as a catalyst, urea as a nitrogen source with ratio of 1: 1 and ZnCl₂ as activating agent with ratio of 2: 1, all respect to the raw material. The mixture was stirred and heated on a hot plate (80°C) for 2 hours. Furthermore, the mixed material is dried in the oven for 2 hours. The mixed material then put into a tubular furnace for carbonization and activation. Tubular furnace is conditioned under nitrogen atmosphere, heated to 250°C within 45 minutes. After reaching the desired temperature, the temperature is maintained for 60 minutes. This is the first stage. Afterward, the temperature was increased to graphitization stage at 900°C and kept the temperature for another 90 minutes under flowing nitrogen. This is the second stage of pyrolysis. The sample was then denoted as G250. Experiments were repeated with the first stage of pyrolysis temperature varied at 350°C and 450°C, denoted as G350 and G450 respectively. Holding time for all treatments are the same. The product was added with HCl 2M and stirred for 30 minutes. Consecutively, the solutions were washed with demineralized water several times until rinsed water reached pH 7. The product then was dried at 105°C for 24 hours to obtain graphene.

2.2. Characterization

Fixed carbon in product was studied using gravimetric analysis. Electron microscopy analysis (SEM and TEM) was performed to study the graphene morphology. Nitrogen adsorption-desorption analysis with Brunauer–Emmett–Teller (BET) calculation method was performed to determine the surface area of the products. Crystallinity of the product was also studied using XRD analysis. To confirm graphitic characteristic of the produced graphene, Raman spectroscopy analysis was performed.

2.3. Electrochemical analysis

Asymmetrical two-electrode configurations were used to evaluate the capacitive performance of the produced graphene. The negative electrodes were prepared by mixing the produced graphene with polyvinylidene fluoride (PVDF) at a weight ratio of 90:10. The above materials were coated onto a 1 cm² stainless steel mesh current collector and dried at 80°C for 8 h. The positive electrodes were prepared by mixing nickel oxide with polyvinylidene fluoride (PVDF) at a weight ratio of 90:10. The materials were coated onto a 1 cm² stainless steel mesh current collector and dried at 80°C for 8 h. Nafion 212 was sandwiched between two electrodes. The test was performed with KOH 6M aqueous electrolyte solution under ambient conditions using Gamry V3000. Electrochemical characteristic of samples was studied using cyclic voltammetry (CV) and electrochemical impedance spectroscopy (EIS) techniques.

3. Results and discussions

The pyrolysis in this experiment consists of two stages, with variation on the temperature of the first stage i.e. 250, 350, and 450°C, followed by the second stage pyrolysis at 900°C. The pyrolysis products were then immersed in HCl 2M for 2 hours to remove Fe impurities. The acid residue was rinsed with aqua dm. The product was then dried at 105°C temperature. To analysis fixed carbon content in this dried sample, the sample was heated at 800°C for 6 hours in the furnace. The remaining unburned sample is ash. The fixed carbon content calculated from the weigh difference between the dried sample and

remaining ash. Result of dried pyrolysis product and fixed carbon content after pyrolysis process are listed in Table 1. To be noted that biomass precursor weight is 3 g.

Table 1. Yield of pyrolysis product and fixed carbon.

Sample	G250	G350	G450
Char (gram)	0.56	0.49	0.37
Fixed Carbon(% w/w)	79.9	90.01	63.37

The results show that temperature of first stage pyrolysis affects to the yield of dried pyrolysis product. The yield decreases with increasing the pyrolysis temperature due to increased loss of condensable material [6]. During thermal decomposition process, biomass components decompose at different temperature ranges. In the first stage (below 200°C), a weight loss of about 10% is caused by loss of water molecules (dehydration). Furthermore, hemicellulose decomposes in range of 150-350°C, cellulose at 275-350°C, whereas the lignin in range of 250-500°C [7]. EFB contains 50.7% lignin [8]. The maximum decomposition of lignin occurs in the temperature range of 350-450°C. Lignin pyrolysis produces more aromatics and char than produce by cellulose. Pyrolysis of the lignin typically produces about 55% char [9]. Therefore, in order to obtain high graphene yield from pyrolysis of EFB, pyrolysis should be carried out at temperature decomposition of lignin. The idea is proved by the results of this study where the highest yield is obtained at first stage pyrolysis temperature of 350°C.

Morphology of graphene resulted from this pyrolysis was analyzed using electron microscopy. Figure 1 shows the SEM and TEM images of the pyrolysis product from EFB with the ratio ZnCl_2 :biomass of 2:1 at various first stage pyrolysis temperature. It is concluded that the temperature of first stage pyrolysis, with advantage on increasing the yield, has insignificant effect on produced graphene. Graphene formation mainly occurs at higher temperatures of second stage pyrolysis. According to Zhang et al. [10], Fe_3C was formed gradually at 700°C and changed to Fe. At higher temperatures, amount of Fe_3C that turns into Fe will increase. As Fe_3C changes to Fe, the activated carbon atoms in Fe_3C layer will diffuse outward to form graphene sheet.

Layer morphology is studied using the TEM analysis in Figure 1(d). The produced graphene seems consist of several layers of graphene. The layers are caused by buildup and assembly of formed template. The few-layers or multilayers graphene-like nanosheets are stacked and folded together, which is beneficial for rapid ion and electron transport during the charge–discharge process of supercapacitors [11].

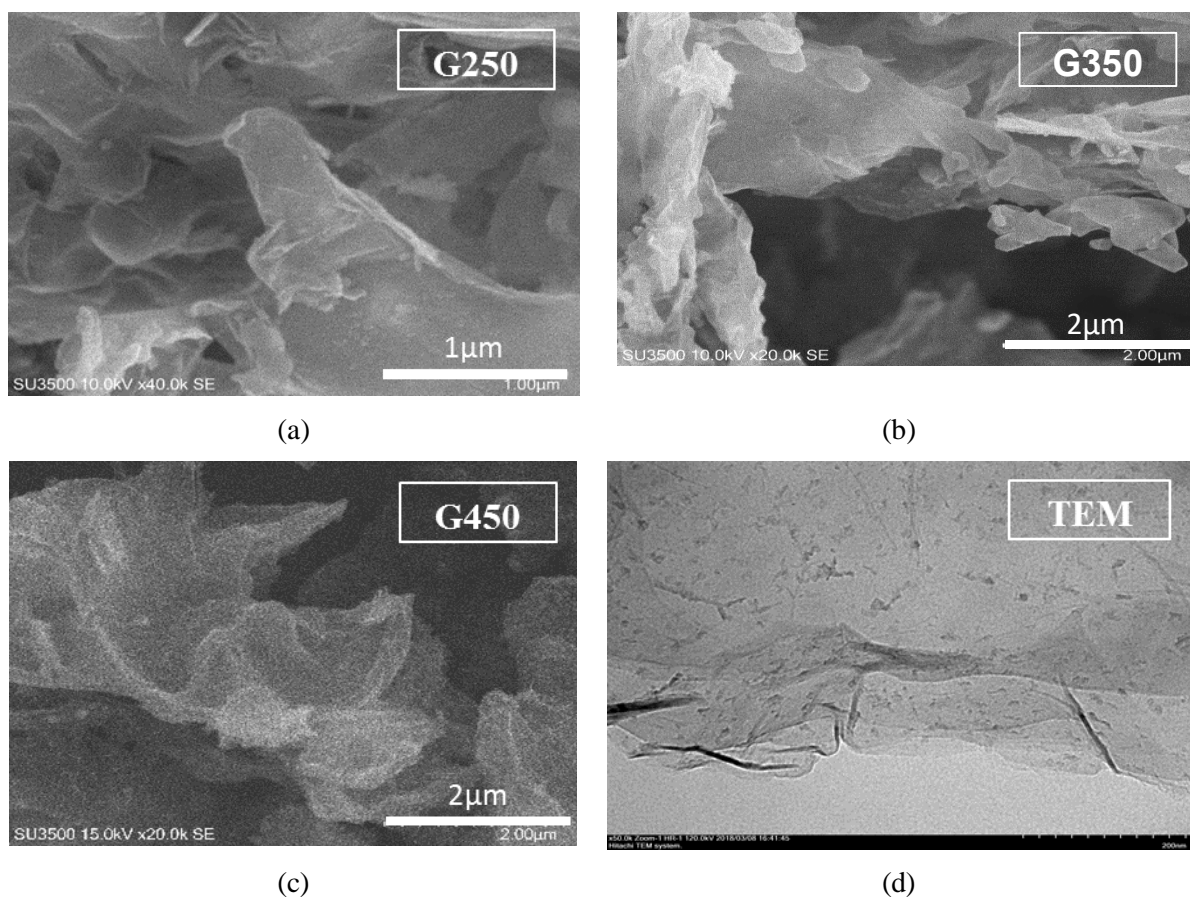


Figure 1. SEM and TEM images of graphene.

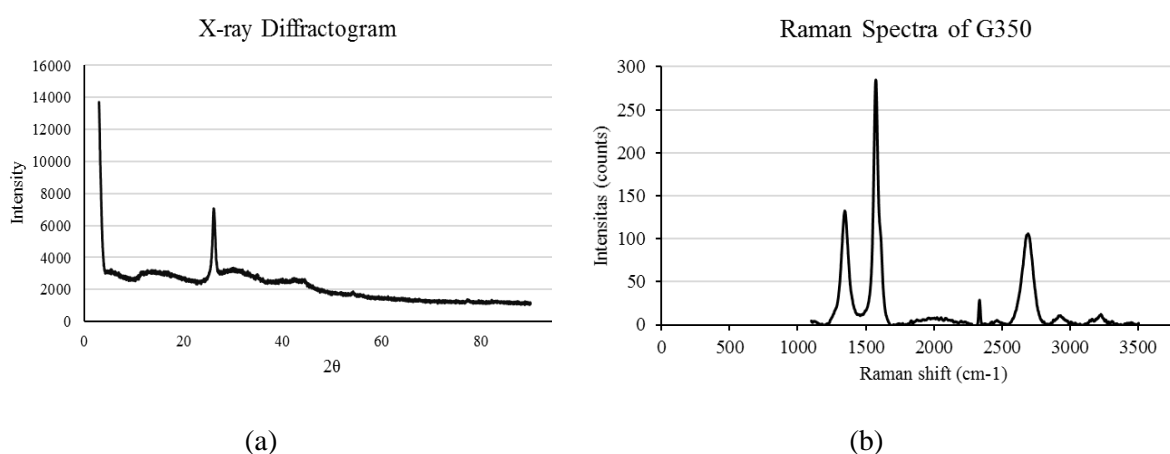


Figure 2. (a) X-ray diffractogram and (b) Raman spectra of G350.

The XRD analysis as shown in Figure 2(a) shows a peak at 26° which indicates graphite structure [11]. The peak on the widened XRD spectrum shows the amorphous carbon structure generated by the destruction process of the initial graphite structure during the pyrolysis process. The resulting carbon structure is an intermediate structure between graphite and amorphous structures called turbostratic structures or random layered lattice structures [12]. The distance between the pseudographitic layers

(d_{002}) calculated using *Match* software is in range of 0.337 - 0.342 nm, in accordance with results of HRTEM analysis.

Further, degree of product graphitization is calculated based on the equation (1) [3]:

$$G = \frac{0,3440 - d_{002}}{0,3440 - 0,3354} \times 100\% \quad (1)$$

Value of 0.3440 in the equation refers to interlamellar distance of the turbostratic graphite (in nm) and 0.3354 is interlamellar distance of a single graphite crystal (in nm). From the calculation, the degree of product graphitization reached 77%. The high degree of graphitization of multiple layers graphene indicates good electrical conductivity [3].

Raman spectroscopy analysis was performed to study further on the produced graphene. The Raman spectra in Figure 2(b) shows the peaks corresponding to the regular graphite lattice mode vibrations. The D-Band is corresponding to the A1g mode which is the vibration of the carbon atoms in the planar termination of the irregular graphite. The G-band determines the E2g mode of 2D graphite, which corresponds to the bonding vibrations of the sp^2 carbon atoms in the hexagonal lattice. Intensity ratio of I_G / I_D is proportional to the crystalline degree of the carbon material. The G and D peak is at a wave number of about 1573 cm^{-1} and 1346 cm^{-1} , respectively. The intensity of G and D peaks depends on the percentage of the graphite domain containing the sp^2 -carbon layer of hybridization in the formed graphene [13]. Based on the Raman spectra, the produced graphene show a regular graphitic character because intensity of G peak is much higher than the D peak. The I_G/I_D value of 2.14 suggests high graphitization degree of the product. The peak in 2690 represents the 2D band. Position and height profile at the 2D peak indicate layering on graphene. Monolayer graphene has 2D peak at 2679 cm^{-1} . The shifting of 11 cm^{-1} to higher wave numbers indicates that our product has 2-4 layers of graphene, in accordance with the results of TEM analysis [13].

Surface area analysis using BET calculations was performed to determine the surface area and pore distribution of graphene. These parameters are important when the carbon material applied as electrode of supercapacitor. The result in Table 2 shows that graphene derived from EFB has significant increment surface area at first stage pyrolysis temperature of 350°C . According to [14] and [15], the surface area decreases at high temperatures treatment due to collapse of micropore into bigger pore. In addition, at high temperatures, the carbon structure shrinks as volatile substances evolve from the structure.

Table 2. Surface area of graphene.

Sample	Surface area ($\text{m}^2 \text{ g}^{-1}$)
G250	290
G350	880
G450	264

Important to note that the graphene surface area can be increased significantly using this two-stage pyrolysis method. In the previous research, surface area analysis of pyrolysis (single stage) EFB at 900°C using FeCl_3 3M catalyst with activating agent ZnCl_2 is $63.12 \text{ m}^2 \text{ g}^{-1}$. In addition, one stage pyrolysis of EFB performed by Nasir [16] at 900°C obtained surface area of EFB is $117 \text{ m}^2 \text{ g}^{-1}$.

Our product of graphene is aimed for supercapacitor. Therefore, electrochemical analysis was performed to test the performance of produced graphene as supercapacitor electrode. Cyclic voltammetry (CV) and electrochemical impedance spectroscopy (EIS) were performed. Cyclic voltammetry was used to observe cell characteristics and capacitance. Supercapacitor cells were prepared for size of $1 \text{ cm} \times 1 \text{ cm}$. The dried product of pyrolysis, acting as a negative electrode, was mounted on a stainless-steel mesh. Nickel oxide, as a positive electrode, was placed on a carbon sheet with a 6M KOH electrolyte. These two electrodes were separated using Nafion 212 membrane.

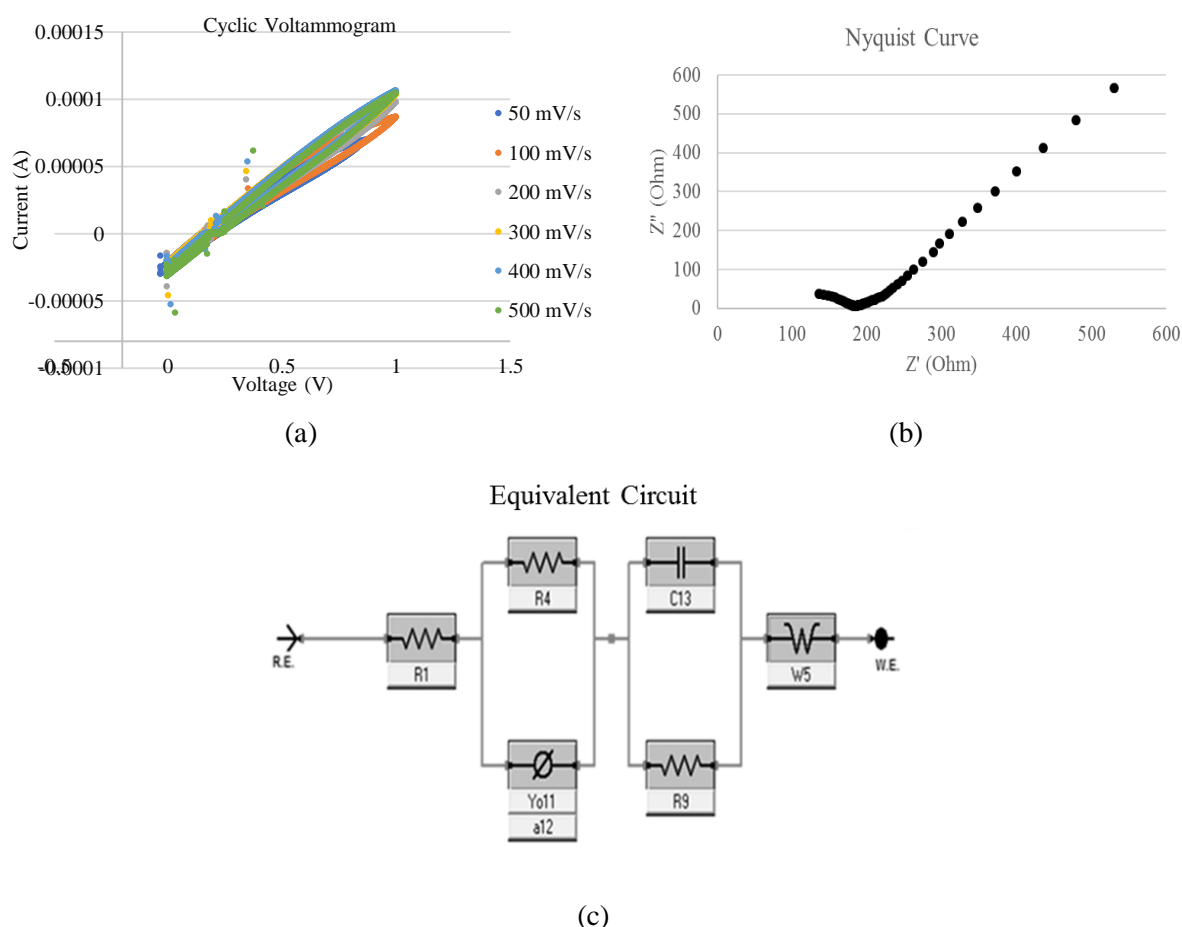


Figure 3. Cyclic voltammogram, nyquist curve and equivalent circuit of supercapacitor from produced graphene.

Under scan rate of 10 mV s^{-1} , a non-ideal CV curves (not quasi-rectangular) was obtained as in Figure 3(a). The curve slope increases with cycle number, indicate the existence of leak current. This leak current may occur due to side reactions between the electrolyte and a functional group in the sample and can be minimized by electrolyte selection [17]. Shape of the curve elongates with increasing scan rates from 50 to 500 mV s^{-1} , result in higher current. This indicates ion transfer barrier from the electrolyte to the electrode surface [18]. Specific capacitance of the produced graphene was calculated from the voltammogram according to following equation:

$$C = \sum |I| \cdot \Delta t / m \Delta V \quad (2)$$

with $I \cdot \Delta t$ is the area of the curve I (A) to t (sec), m (gram) is the mass of active ingredient in the cell, ΔV (V) is operating range of cell voltage. Obtained capacitance for G350 sample is 0.054 F g^{-1} . This low capacitance is supposed due to cell resistance. Therefore, electrochemical impedance spectroscopy (EIS) analysis to the cell was performed.

The EIS result is shown in a Nyquist plots (Figure 3(b)). Equivalent electrical circuit model in Figure 5c was used to describe electrochemical impedance in the cell. Ideal supercapacitor shows a 90° straight line in low frequency as the capacitance is dominant. Good supercapacitor indicated by Warburg impedance close to the 90° straight line. In this study, however, Nyquist plot show a straight line of 45° in low frequency as supposed in the conventional capacitors. This indicates a considerable resistance value of active species diffusion from electrolyte to electrode. In medium frequency, there are electrolyte interphase resistance within the pores of electrodes with domino effect. In high frequency, the real axis intercepts are equivalent series resistance (ESR). Semicircle diameter of the impedance loop represents

the charge transfer resistance in the electrode material. The equivalent electrical circuit shown in Figure 3(c) is modeled by the Schrödinger coupled nonlinear equation (CNLS). The whole capacitor circuit is constituted by R1, R4, CPE, C13, R9 and W5. R1 is the sum of the contact resistance and material resistance (electrode, electrolyte and separator). W5 is the Warburg resistance which is related to the ion diffusion/transport in the electrolyte. The resistance parameter of R4 and R9 are interface resistances for mass transfer of electrolytes into the electrode pores [11]. The capacitive element of C13 is related to capacitors formed during charge-discharge process and CPE is not ideal capacitor. Parameters of the equivalent electrical circuit model are presented in Table 3.

Table 3. Impedance parameters of graphene cell

Parameter	Unit	Value	Parameter	Unit	Value
R1	Ohm	9.395×10^{-5}	Yo11	$S*s^a$	3.952×10^{-3}
R4	Ohm	186.1	a12		5.781×10^{-1}
W5	$S*s^{(1/2)}$	1.03×10^{-2}	C13	F	4.959×10^{-2}
R9	Ohm	1.26×10^3			

The interface resistance of R4 and R9 are high. Graphene which is a hydrophobic material has low interaction with aqueous based electrolyte, increasing interface resistance. Surface modifications by hydrophilizing agents are proposed to make the graphene surface more hydrophilic [19]. This modification is still being studied further in our laboratory. Internal resistance in the electrode paste matrix can be reduced by increasing percolation. Addition of 10 to 20% conductive carbon filler is proposed. Current collectors and conductive pastes contribute to the weight that could not be ignored in the device. Any non-capacitive weights in cells reduce device performance. As a result, the additive paste used should be as minimal as possible and optimal, as well as the current collector used should be thin and light [20]. Proper cell sealing is also a key component of cell assembly. Evolution of gases from electrolyte degradation, corrosion, and oxidation of electrode and packaging surfaces could be a problem [21]. A tight seal will prevent water and gas molecules from entering the cell. Another major reason for proper sealing is to prevent shunt resistance between electrodes and adjacent cells. The shunt current significantly increases self-discharge and reduces the efficiency of the device. Bad seals will be damaged over time which causes degradation and short circuit [22]. Heat can be applied to make the plastic shrink and tightly seal the cell.

4. Conclusion

Yield of graphene synthesis from oil palm empty fruit bunches can be increased by using two-stage pyrolysis method. In addition, the pyrolysis temperature at the first stage of heating affects surface area and fixed carbon in the product. The highest graphene yield was obtained when the first pyrolysis temperature at 350°C, which is about 70%.

5. Acknowledgement

This work is supported by Badan Pengelola Dana Perkebunan Kelapa Sawit, funding year of 2018. We deeply thank Prof. Wuled Lenggoro, Ferry Faizal, and Yuria Watanabe for insight and helpful supports.

6. References

- [1] Hernández M A, Romero J, Jaime C, Pulido J L and Cabeza I O 2017 *Chem. Eng. Trans.* **58** 541-6
- [2] Castro N, Guinea A H, Peres N M R, Novoselov K S and Geim A K 2009 *Rev. Mod. Phys.* **81** 109-162
- [3] Chen F, Yang J, Bai T, Long B and Zhou X 2016 *J. Elec. Chem.* **768** 18-26
- [4] Tan Y B and Lee J M 2013 *J. Mat. Chem. A* **1** 14814-43
- [5] Shams S, Zhang L Z, Hu R, Zhang R and Zhu J 2015 *Mat. Lett.* **161** 476-9

- [6] Giudicianni P, Stefania P, Grottola C M, Stanzione F Faugno S, Fagnano M, Fiorentino N and Ragucci R 2017 *Chem. Eng. Trans.* **5** 500-5
- [7] Chen W and Kuo P A 2010 *Energy* **35** 2580-6
- [8] Chang G, Huang Y, Xie J, Yang H, Liu H, Yin X and Wua C 2016 *Ener. Conv. Man.* **124** 587-97
- [9] Soltes E J and Elder T J 1981 *Pyrolysis* (New York: CRC Press)
- [10] Zhang S, Zeng M, Li J, Xu J and Wang X 2014 *J. Mat. Chem. A* 2014 **2** 4391-7
- [11] Sun L, Tian C, Li M, Meng X, Wang L, Wang R, Yin J and Fu H 2013 *J. Mat. Chem. A* **1** 6462-70
- [12] Manoj B and Kunjomana A G 2015 *IOP Conf. Ser.: Mater. Sci. Eng.* **73** 012096
- [13] Sahu V, Grover S, Tulachan B, Sharma M, Srivastava G, Roy M, Saxena M, Sethy N, Bhargava K, Philip D, Kim H, Singh G, Singh S K, Das M and Sharma R K 2015 *Elec. Acta.* **160** 244–53
- [14] Kaghazchi T, Kolur, N A and Soleimani M 2010 *J. Ind. Eng. Chem* **16** 368–374
- [15] Yang T and Lua A C 2006 *Mat. Chem. Phys.* **100** 438–44
- [16] Nasir S, Hussein M Z, Yusof N A and Zainal Z 2017 *Nanomater.* **7** 1-18
- [17] Gu W, Peters N and Yushin G 2013 *Carbon* **53** 292-301
- [18] Yu A, Chabot V and Zhang J 2013 *Electrochemical Supercapacitors for Energy Storage and Delivery* (New York: CRC Press) p 66
- [19] Akkarachainona N, Rattanawaleedirojn P, Chailapakula O and Rodthongkumb R 2017 *Talanta* **165** 692-701
- [20] Demarconnay L, Raymundo-Piñero E and Béguin F 2010 *Electrochem. Commun.* **12** 1275-8
- [21] Simon P and Gogotsi Y 2008 *Nat. Mater.* **7** 845–54
- [22] Kotz R and Carlen M 2000 *Elec. Acta* **45** 2483-98